OTELO Survey: Properties of X-ray emitters in the Groth Field
I. Optical counterparts and morphological classification

M. Pović[1,*], M. Sánchez-Portal[2,**], A. M. Pérez García[1], A. Bongiovanni[1], J. Cepa[1,3], J.A. Acosta-Pulido[1], E. Alfaro[4], H. Castañeda[1], M. Fernández Lorenzo[1], J. Gallego[5], J. I. González-Serrano[6], J. J. González[7] and M. A. Lara-López[1]

Abstract We present results from the study of optical broadband and X–ray properties of a large sample of active galactic nuclei (AGN) in the Groth-Westphal Strip (GWS) field. In order to determine the morphology of all objects, we obtained different structural parameters. Combining these parameters with other optical/X–ray properties, we were searching for possible correlations between them, which could point out some of the AGN characteristics (see part II, Sánchez-Portal et al.).

1 Observational data

1.1 X-ray and optical data

We have used *Chandra* public data of three ACIS-I pointings (PI is K. Nandra) in the deep 200ksec, small ~ 0.2 square degrees area survey. Data were processed using CIAO v3.3.0.1. Five energetic bands have been selected in the range 0.5-7 keV. The final catalog contains 639 sources (Sánchez-Portal et al., 2007).
Using 4.2m William-Herschel Telescope (La Palma, Canary Islands), three areas have been observed in the GWS field with broadband BVRI filters, with the total exposure time ranging from 8400 to 10000 sec and a total covered area of ~ 0.18 deg^2. Our limiting magnitudes are B 25, V 25, R 24.5 and I 23.5. The final catalog contains ~ 45000 objects (Cepa et al., 2008).

[1]Instituto de Astrofísica de Canarias, 38205 La Laguna, Spain, [2]Herschel Science Centre, ESAC/INSA, Madrid, Spain, [3]Departamento de Astrofísica, Universidad de La Laguna, 38205 La Laguna, Spain, [4]Instituto de Astrofísica de Andalucía-CSIC, Granada, Spain, [5]Departamento de Astrofísica y CC. de la Atmósfera, Universidad Complutense de Madrid, Madrid, Spain, [6]Instituto de Física de Cantabria, CSIC-Universidad de Cantabria, Santander, Spain, [7]Instituto de Astronomía UNAM, México D.F, México
[*]e-mail: mpovic@iac.es
[**]e-mail: miguel.sanchez@sciops.esa.int

1.2 The catalogue of optical counterparts

In order to build a sample of X–ray emitters with optical counterparts, we performed cross–matching of the X–ray and optical catalogues using the TOPCAT tool (Taylor, 2005).We chose a maximum search radius of 2 arcsec after carrying out several tests considering a maximum searching distance of 1 to 5 arcsec with a bin of 0.5 arcsec. We detected 340 optical counterparts of the X–ray sources. The completeness of our detection is 98.3% ($\sim$ 1 object lost), while the reliability is 87.3% ($\sim$ 39 potentially false matchings).

1.3 X-ray number counts

We calculated the cumulative number count distributions (logN-logS) per deg^2 in the soft band in order to test the reliability of our source detections. We compared our distribution with that computed by Nandra et al. (2005) and those provided by other deep X–ray surveys (see Fig. 1). For our sample two curves have been computed, one for the complete sample of X–ray detections and the other only for the X–ray detections that have optical counterparts. In general, at our flux limit the number counts of our complete X–ray sample are in good agreement with Nandra et al. (2005) and other surveys.

1.4 X-ray colour-colour diagram

We represented detected X–ray sources on the X–ray colour-colour diagram (Fig. 2), superposing them on an absorbed power low model grid. Hardness ratios are computed as: HR($\Delta_1 E$,$\Delta_2 E$) = (CR($\Delta_1 E$) - CR($\Delta_2 E$))/(CR($\Delta_1 E$) + CR($\Delta_2 E$)), where $\Delta_1 E$ y $\Delta_2 E$ are different energy bands and $CR(\Delta_n E)$ is the count rate in a given energy band. Photon index is varying between 0 and 3 with a bin of 0.5 (dashed lines from up to down) and a log of absorption column density between 20 and 24 in steps of 0.5 (solid lines from left to right). Most of the sources are located inside the grid, suggesting that their spectrum can be properly represented by power low

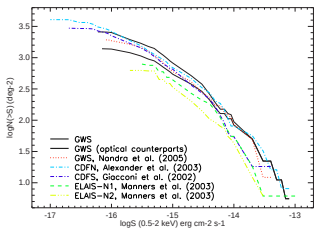

Fig. 1 Cumulative logN-logS functions for the Groth field in the soft band, for all detected X–ray sources (black thick solid line) and for X–ray sources with optical counterpart (black thin solid line).

with different absorption column densities, but still a group of sources are located outside the model grid. For the fitting of these objects probably more components should be added.

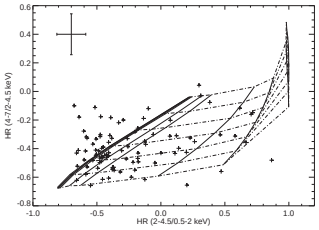

Fig. 2 X–ray colour-colour diagram based on 2–4.5/0.5–2keV vs. 4–7/2–4.5keV hardness ratios. X–ray sources (crosses), from the complete X–ray catalogue, are represented and superposed on an absorbed power law model grid. Median error bars are represented in the upper left corner of the diagram.

2 Structural parameters and morphological classification

Using SExtractor (Bertin & Arnouts, 1996) and GIM2D (Simard, 1998) we have computed several morphological parameters of the optical counterparts, including concentration and asymmetry indexes, residual parameter, bulge-to-total ratio, Sérsic index and SExtractor CLASS_STAR parameter for the compact object selection. To check the reliability of all obtained structural parameters we also applied the visual inspection for all objects, observing different types of galaxy profiles and its counter diagrams obtained by imexamine IRAF tool (see Fig. 4). We have seen that when dealing with faint objects ($R < 24$) with small isophotal area (< 200 pixels), the combination of the concentration index with the asymmetry index gives us the most reliable morphological classification (see Fig. 5). Five categories or groups are created associating ranges of values of C with Hubble types:

$$\begin{aligned} 0{:}\ C \geq 0.7 \text{ or CLASS\_STAR} \geq 0.9 &\quad \rightarrow \text{Compact objects} \\ \text{I}{:}\ 0.45 \leq C < 0.7 &\quad \rightarrow \text{E, E/S0 y S0} \\ \text{II}{:}\ 0.3 \leq C < 0.45 &\quad \rightarrow \text{S0/S0a-Sa} \\ \text{III}{:}\ 0.15 \leq C < 0.3 &\quad \rightarrow \text{Sab-Scd} \\ \text{IV}{:}\ C < 0.15 &\quad \rightarrow \text{Sdm-Irr} \end{aligned}$$

The first group is populated by elliptical and lenticular galaxies, whose profiles do not show any trace of disc or spiral arms (see Fig. 4), the second group includes very early spiral type galaxies which show signs of spiral arms. The third group comprises spiral galaxies while the fourth includes late type spirals and irregular galaxies, that show almost no regular form in their profiles. All galaxies, even those in the first group (elliptical and lenticular) have a concentration index $C < 0.7$, while all objects with $C \geq 0.7$ have been classified by SExtractor as compact ones, with the CLASS_STAR parameter ≥ 0.9.

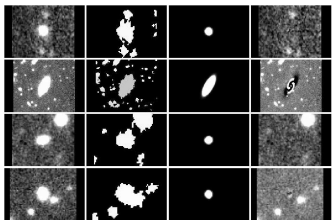

Fig. 3 Four sample images of the GIM2D decomposition procedure. From left to right: subimages of objects to be fitted (obtained from the scientific image), mask subimages, subimages after modelling and residual subimages (obtained from the original image after subtracting the model)

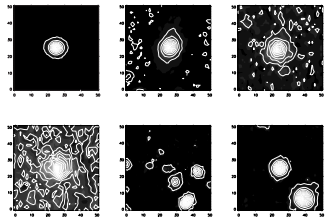

Fig. 4 Sample of different Hubble type galaxies and their contour diagrams; Up: Left: Group I (E/S0), Center: group II (Early type spiral), Right: group III (Spiral); Down: Left, group III (Spiral), Center: group IV (Irr) , Right: compact object (CLASS_STAR > 0.9). All objects are located in the center of the images.

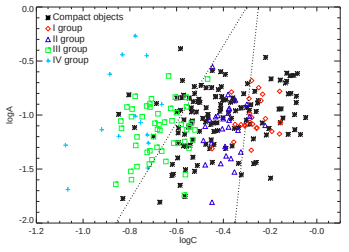

Fig. 5 Asymmetry vs. concentration index. Dotted lines represent Abraham et al. (1996) limits between E/S0, spiral and Irr galaxies, using HST data. We can notice a shift of our late type galaxies to lower C values, due to a seeing effect in our ground-based data.

References

Abraham, R. G., et al. 1996, ApJ, 107, 1
Alexander, D. M., et al. 2003, Astronomische Nachrichten, 324, 8
Bertin, E. & Arnouts, S. 1996, A&AS, 117, 393
Cepa, J. et al. 2008, A&A, (accepted)
de Ruiter, H. R., et al. 1977, A&AS, 28, 211
Giacconi, R., et al. 2002, ApJS, 139, 369
Manners, J. C., et al. 2003, MNRAS, 343, 293
Nandra, K., et al. 2005, MNRAS, 356, 568
Sánchez-Portal, M., et al. 2007, RevMexAA, 29, 175
Simard, L. 1998, ASPC, 145, 108
Taylor, M. B. 2005, ASPC, 347, 29

We would like to thank Laura Tomás who kindly provided us with her software for diagnosis of hardness ratios using model grids.